

Synthesis and Characterization of Core-Shell Particles Containing a Perfluoroacrylate Copolymer Rich in the Shell

Yang Tingting,¹ Peng Hui,¹ Cheng Shiyuan,¹ In Jun Park²

¹School of Chemistry and Materials Science, Hubei University, Wuhan 430062, China

²Department of Chemistry Engineering, Korea Research Institute of Chemistry Technology, Taejon 305-606, South Korea

Received 27 January 2006; accepted 21 October 2006

DOI 10.1002/app.25679

Published online 8 March 2007 in Wiley InterScience (www.interscience.wiley.com).

ABSTRACT: A simple synthetic method for preparing the core-shell latex particles containing fluorinated shell was presented. Polymerization was achieved by a low-shear monomer-starved emulsion polymerization process, thus facilitating mobility and subsequent polymerization of perfluoroacrylate (FA) along with methyl methacrylate (MMA) and *n*-butyl acrylate (nBA) monomers. The structure and thermal behavior of the resulting perfluoroacrylate copolymer were investigated by FTIR, NMR, and DSC. Furthermore, PCS, TEM as well as SFM, were carried out to charac-

terize the surface morphology of the particles. These studies illustrated that the incorporation of FA into MMA/nBA particle morphologies facilitated surface phase separation during coalescence, resulted in F-containing film-air interfaces. Thus, surface properties with a significant increase in the contact angles could be produced. © 2007 Wiley Periodicals, Inc. *J Appl Polym Sci* 104: 3277–3284, 2007

Key words: perfluoroacrylate; surface morphology; hydrophobicity; contact angles

INTRODUCTION

The incorporation of fluorine-containing monomers into polymeric systems has been of considerable interest because of the fact that their presence may introduce a number of unique physical and chemical properties, such as high thermal and photochemical resistance, water and oil repellency, and self-cleaning.^{1–4}

Although it is advantageous to synthesize and handle F-containing polymers via emulsion polymerization, their incorporation into colloidal particles is not straightforward mainly because of the immiscibility between hydrophobic C–F entities and continuous aqueous phase resulting from large surface tension differences. Several attempts^{5–10} such as organic cosolvents, high shear, homogenizers, and fluorinated surfactants were utilized to facilitate monomer diffusion through an aqueous phase. Another approach was to incorporate perfluoroacrylate polymers into colloidal particles because of their excellent reactivity with acrylates and good adhesion to matrices.^{9,11–15}

The surface, which occupied by a close-packed array of $-\text{CF}_3$ groups to present the self-assembled monolayer of perfluoroalkyl chains, possesses the lowest surface energy attainable. In fact, if most of long-side-chain perfluoroalkyl groups could be made to orientate and occupy the surface, the highest density of the uniformly organized $-\text{CF}_3$ groups can be achieved while reducing the overall fluorine content used. These are achieved (i) through appropriate synthesis of segmented, block, or graft copolymers structures that favor surface segregation,^{9,14,15} or (ii) by blending with nonfluorinated polymers,¹⁶ which will eventually phase separate, and (iii) through the migration of the fluorinated side chain in the shell.^{17–19} The ultimate goal in designing the structured particles is to use a little FA and to obtain the most of the $-\text{CF}_3$ groups array at final film/air interfaces, which will then be more hydrophobic than an entirely hydrogenated films.

Despite numerous difficulties and challenges in incorporating F-containing species into colloidal dispersions, there are also opportunities. This study presents a simple synthetic method, which utilizes monomer-starved conditions implemented during a semicontinuous emulsion polymerization process to produce core-shell latex particles containing fluorinated shell. The second part of this study concerns the core-shell particles morphology.

Correspondence to: C. Shiyuan (scheng@public.wh.hb.cn).

Contract grant sponsor: Specialized Research Fund for the Doctoral Program of Higher Education of China; contract grant number: 20050512001.

TABLE I
Recipes and Conversions for the Core-Shell Latex Particles Synthesis

Step	Composition (g)	Run 1	Run 2	Run 3	Run 4	Run 5	Run 6	Run 7	Run 8
Seed (batch)	MMA	3.0	3.0	3.0	3.0	3.0	3.0	3.0	3.0
	n-BA	3.0	3.0	3.0	3.0	3.0	3.0	3.0	3.0
	AMPSNa	0.25	0.5	0.5	0.5	0.5	0.5	0.5	0.5
	KPS	0.05	0.05	0.05	0.05	0.05	0.05	0.05	0.05
	H ₂ O	65	65	65	65	65	65	65	65
Second slow step	FA	0.8	0.0	0.1	0.2	0.6	0.8	1.2	0.6
	VTES	0.4	0.4	0.4	0.4	0.4	0.4	0.4	0.0
	MMA	7.0	7.0	7.0	7.0	7.0	7.0	7.0	7.0
	n-BA	7.0	7.0	7.0	7.0	7.0	7.0	7.0	7.0
	KPS	0.05	0.05	0.05	0.05	0.05	0.05	0.05	0.05
	H ₂ O	10	10	10	10	10	10	10	10
Conversion (%)		95.4	96.1	97.8	96.2	96.9	94.0	93.2	97.2

EXPERIMENTAL

Materials

Perfluoroacrylate ($\text{CH}_2=\text{CH}_2\text{COOCH}_2\text{CH}_2(\text{CF}_2)_7\text{CF}_3$, 97%) was purchased from Aldrich. And sodium 2-acrylamide-2-methyl propanesulfonate (AMPSNa) was a gift from Lutozol Lmt. The two materials are used directly. MMA and nBA were dried with CaH_2 , and then vacuum-distilled. Vinyltriethoxysilane (VTES) was filtered prior to use. Potassium persulfate (KPS) was purified by recrystallization. Deionized water was obtained by ion exchange.

Polymerization process

All latex particles were synthesized under monomer-starved conditions using semicontinuous emulsion polymerization and following a procedure was described in Table I. Typically, the polymerization was performed in a 0.25-L four-necked kettle equipped with mechanical stirrer, thermometer, reflux condenser, and inlet system of nitrogen. Deionized water 60 g, MMA 3.0 g, nBA 3.0 g, and AMPSNa 0.5 g were charged into the kettle at room temperature followed by carefully removing oxygen by purged nitrogen for 30 min. Then, the resulting pre-emulsion was added initiator KPS 0.05 g dissolved in a small amount of water (5 g) and heated to 74°C. After the autoacceleration process was finished, the rest monomers including MMA 7.0 g, BA 7.0 g, VTES 0.4 g, and a certain amount of FA, together with the initiator 0.05 g dissolved in water 10 g, and was slowly dropped into the reaction system within the time scale of 2 h, respectively. The total conversion of monomers was determined gravimetrically.

Preparation of thin copolymer films

By casting method, films were prepared from a dilute emulsion (~ 10 wt % solid content) on new-cleaned PTFE plates and allowed to dry at room

temperature. The peeled films were immersed into deionized water at a present time (24 h) to remove possible remnants of reactive surfactant. And in the case of scanning force microscopy (SFM) measurements, the samples were prepared by casting coating from a dilute emulsion of polymer with the weight concentration of 10^{-5} – 10^{-6} g/g onto a freshly cleaved mica surface. To further promote the migration of perfluorinated side chains, all films were annealed above the T_g and then kept in an oven at room temperature under vacuum.

Structural characterization

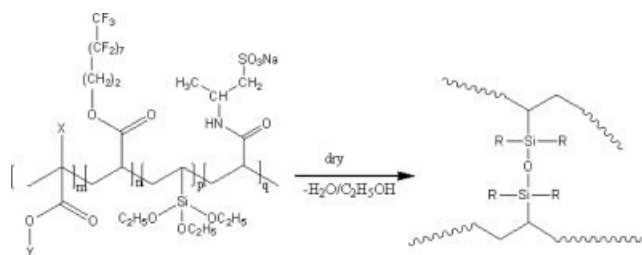
The infrared spectrum of the neat, powdered samples was recorded on an FTIR spectrophotometer (PerkinElmer SpectrumOne). Measurements of ^1H , ^{19}F , and ^{29}Si NMR were carried out on an INOVA 600 MHz spectrometer at 25°C using chloroform-*d* as the solvent. Chemical shifts for ^{19}F NMR are stated downfield from trifluorotrchloroethane ($\text{C}_2\text{F}_3\text{Cl}_3$). Thermal analysis of the resulting FA copolymers was conducted under a PerkinElmer DSC7 instrument with a temperature gradient ranging from –60 to 200°C at 20°C/min.

Latex characterization

The diameters (D_w) of the synthesized particles were studied on Photo Correlation Spectroscopy (Auto Size Loc-Fc963, Malven). PDI referred to the particle dispersity index, and the smaller the PDI values, the narrower the distribution of particle size was. The particle numbers per micro liter water (N_p) was calculated from the following equation:

$$N_p = 6WX/\rho\pi D_w^3 V \quad (1)$$

where W is the original monomer weight, ρ is polymer density fixed 1.1 g/mL, V is the volume of water, and X is the total conversion of monomers.



Scheme 1 Crosslinking reaction between perfluorinated acrylates copolymers during the thermal curing process. For this study, m , n , p , and q represent the weight concentrations ratio for comonomers. And R represents the $-\text{OH}$ group or the $\text{Si}-\text{O}-\text{Si}$ bond, X represents H or $-\text{CH}_3$ and Y represents $-\text{CH}_3$ or $-\text{CH}_2\text{CH}_2\text{CH}_2\text{CH}_3$.

The morphology of latices was characterized by transmission electron microscopy (TEM), which was taken with a TEX-100SX instrument operating at 10 KV. The scanning force microscopy (SFM) measurements were obtained with a Nanoscope IIIa (Digital Instrument, Santa Barbara, CA). All measurements were made in the tapping mode.

Contact angle measurements

Contact angles (θ) data of latex films were taken by Wilhelmy method at 25°C using a Krüss interface tension meter (Krüss GmbH, Hamberg, Germany). The sample was hold in the microbalance and progressively immersed into water, then, conversely receded to its original position at a constant rate of 0.5 mm/s. The analysis of the wetting force data yielded two contact angles, which were an advancing CA (θ_a) and a receding CA (θ_r).

RESULTS AND DISCUSSION

Synthesis of core-shell latex particles

As indicated in the Introduction, the synthesis of F-containing colloidal dispersions may be troublesome because of the poor miscibility between aqueous phase and monomers in the presence of perfluoroacrylate. To overcome these difficulties, we developed a simple synthetic procedure that allows the incorporation of FA into MMA/nBA copolymer particles under monomer-starved conditions using soap-free emulsion polymerization. And the auxiliary comonomer, AMPSNa, was not physically but chemically bonded to the surfaces of latex to impart stronger stabilities.

The results, listed in Table I, showed that the monomer conversion could reach above 95% after polymerization. Therefore, it was anticipated that the chemical compositions of latex particles were not much different from those of monomers. Notably, the lowest values, 93.2% of monomer conversion

was attained when the highest FA concentration in the formulation. The difference of interface energy between polymer and the monomer phase increased with FA concentration increasing, which resulted that the wetting process of FA on the polymer surface to polymerize became more difficult, thus, finally, more gel occurred.

The crosslinkage of the final films took place between the reactive ethoxy groups located on silicon atoms. Upon heating above 100°C , losing water and ethanol, the $\text{Si}-\text{O}-\text{Si}$ bonds formed as shown in Scheme 1. There was an increase in hydrophobicity as a result of the loss of the functional ethoxy groups, which were relatively more hydrophilic. As we known, the structure of the surface layer may undergo surface penetration and surface reconstruction when exposed to polar solvents.^{20,21} The solvent-induced surface rearrangement may be controlled by crosslinking to immobilize the oriented perfluoroalkyl groups to form a permanent low-energetic surface.

Structural characterization

In an effort to determine the FA was indeed incorporated into MMA/nBA copolymer particles, NMR and FTIR were utilized. In addition, the thermal behavior was checked by DSC. The FA copolymer powder was precipitated by acetone, and then purified by a selectively extraction in $\text{C}_2\text{F}_3\text{Cl}_3$ for 24 h, which allowed separation that possibly presented unreacted FA monomer and its homopolymer.

As shown in Figure 1, the FTIR spectrum suggested an intense $\text{C}=\text{O}$ stretching absorption at 1730 cm^{-1} and additional functional groups such as $-\text{CH}_2$ and $-\text{CH}_3$ (a strong peak at $2800\text{--}3000\text{ cm}^{-1}$). It was resulted from the fact that nBA, MMA, and FA all contain $-\text{CH}_2$ and $\text{C}=\text{O}$ groups. And the first wide region of noteworthy lied between 1100 and 1300 cm^{-1} , which was dominated by bands

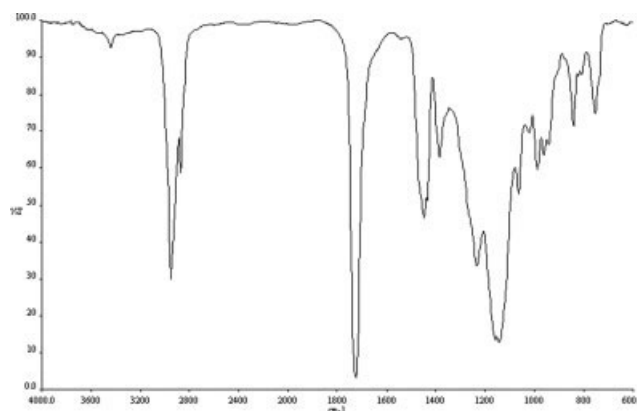


Figure 1 FTIR spectrum of the FA copolymer latex films (run 6).

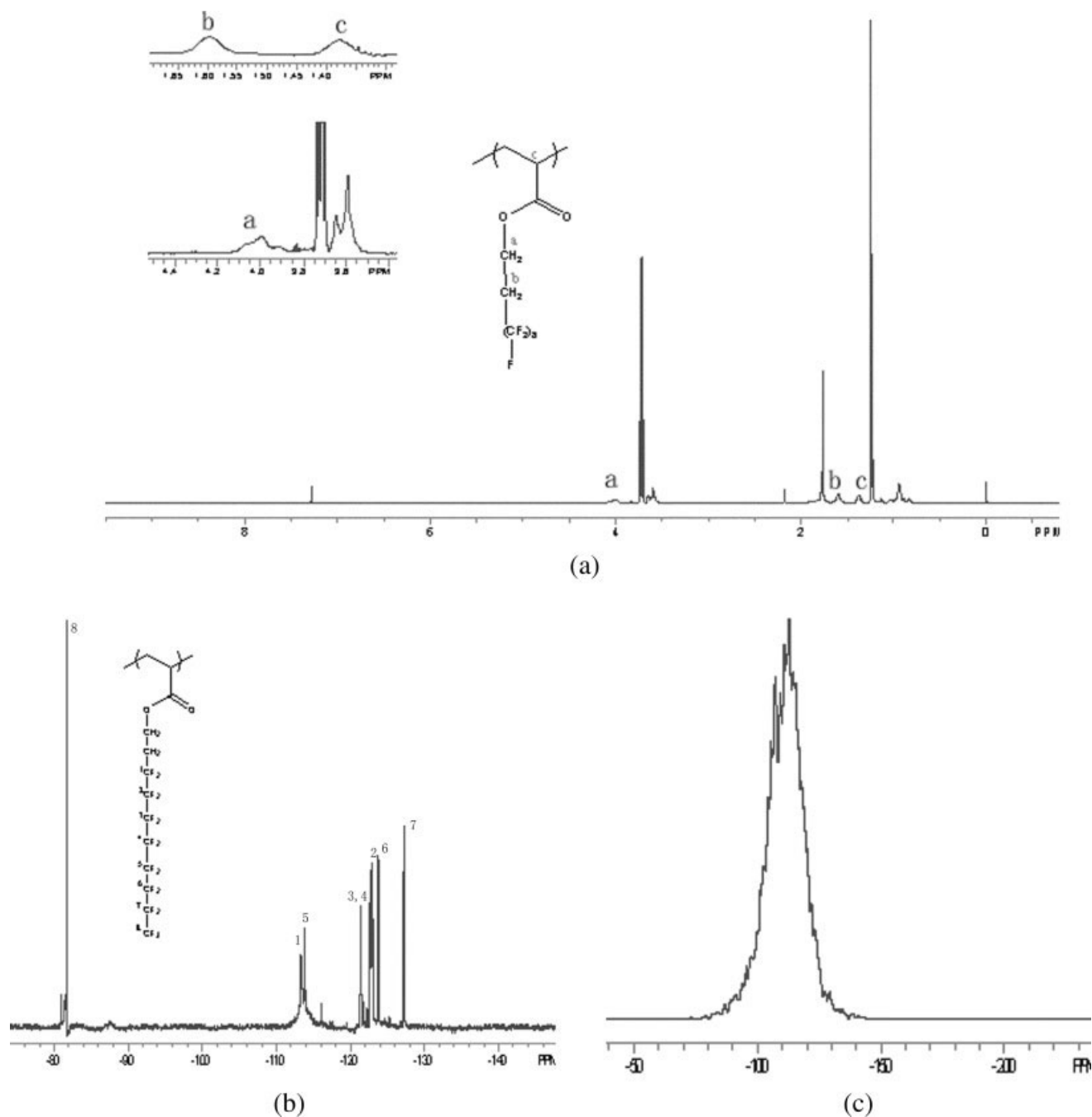


Figure 2 (a) ^1H NMR spectrum of the perfluorinated copolymer (run 6), (b) ^{19}F NMR spectrum of the perfluorinated copolymer (run 6), and (c) ^{29}Si NMR spectrum of the perfluorinated copolymer (run 6).

associated with motions of the CF_2 group at 1150, 1260 cm^{-1} , and the $\text{Si}-\text{O}-\text{Si}$ bonds at 1079 cm^{-1} . In addition, the band at 1560 cm^{-1} was attributed to stretching and bending of carbon skeleton of the fluorocarbon helix. In the second region, there were two medium bands at 660 and 710 cm^{-1} , which resulted from a combination of rocking and wagging vibration of CF_2 groups.

Figure 2(a) was a typical ^1H NMR spectrum of the resulted FA copolymer. A $-\text{COOCH}_2-$ peak at $\delta 4.034$ ppm (t, 2H) because of the FA units in the

polymer chain was observed, and another peak at $\delta 1.813$ ppm (t, 2H) was assigned to $R_f\text{CH}_2-$. The molecular structure of FA was so similar to MMA and nBA that the other proton peaks almost overlapped each other. The incorporation of fluorinated monomers into the latex particles was confirmed by ^{19}F NMR depicted in Figure 2(b) by evaluating the three different kinds of peak intensities at -81.5 ppm (t, 3F) of end $-\text{CF}_3$ group, -114.5 ppm (t, 2F) of $-\text{CH}_2\text{CF}_2-$ group, and -121 to -125 ppm of $-(\text{CF}_2)_5$, respectively. And the ^{29}Si NMR spec-

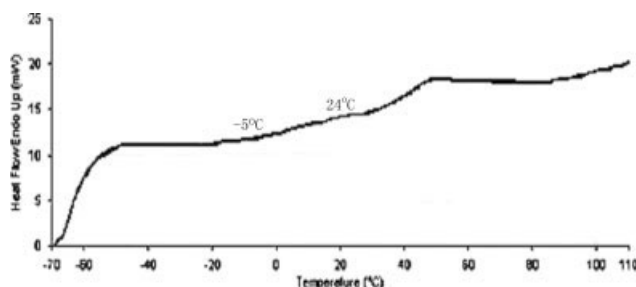


Figure 3 DSC curve of the perfluorinated copolymer (run 6).

trum [Fig. 2(c)] of the resulted copolymers clearly supported the crosslinkage Si—O—Si groups. In addition, two different kinds of silicon resonances at 105 and 120 ppm originating from Si under different crosslinkage extent were observed.

As showed in Figure 3, the representative DSC trace of a FA copolymer indicated two distinctive glass transition regions, one at around $\sim -5^\circ\text{C}$ and the other broad one at 24°C . The first glass transition temperature, T_g , was assigned to MMA/nBA copolymer. It is known that FA homopolymer is semicrystalline showing the first-order transition at 75°C , but the small amount of FA (<10 wt %) in the compositions was not enough to induce the sharp difference of 30°C between two T_g s. And the increase of T_g was not simply attributed to the incompletely crosslinkage by VTES, either. Notably, even if at the macroscopic scale the FA copolymer surfaces were homogeneous and clear, the analysis showed that all samples exhibited two T_g s.

Latex characterization

To determine if indeed FA existed as a separate colloidal particle, the colloidal characteristics (mean particle diameter, particle dispersity index, and particle numbers) of the core-shell particles were analyzed and the data was listed in Table II. As seen, the particle size of MMA/nBA/FA ranged from 121

TABLE II
Diameters of the Particles Measured by SFM and Colloidal Characteristics (Mean Particle Diameter, Particle Dispersity Index, and Particle Numbers) for the Synthesized Latex Particles

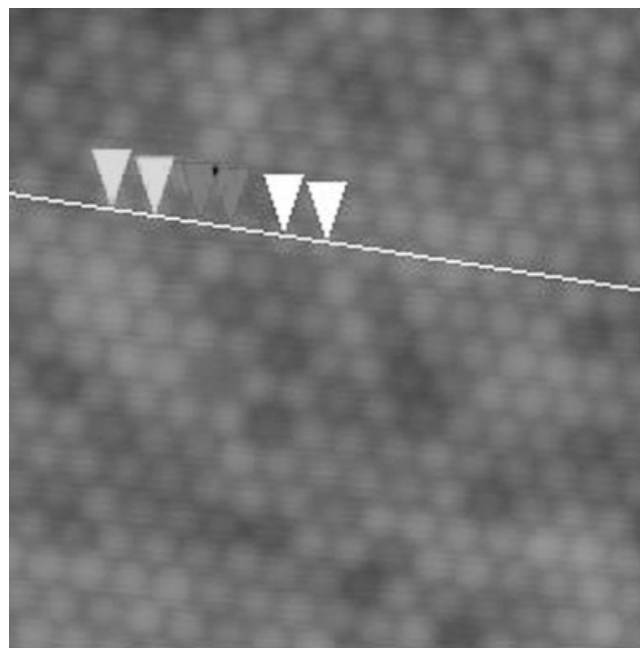
Samples	D_w (nm) ^a	D_w (nm) ^b	PDI	$N_p \times 10^{-15}$ (mL of H ₂ O)
Run 1	139.56	160.4	0.048	0.123
Run 2	126.56	157.4	0.086	0.135
Run 3	140.28	163.2	0.070	0.118
Run 5	121.99	151.8	0.082	0.149
Run 6	138.42	160.4	0.252	0.149

^a Measured by SFM.

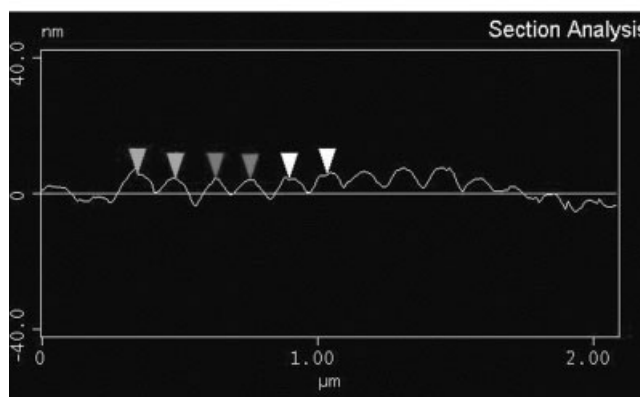
^b Measured by PCS.

to 139 nm with monomodal distribution of the particles regardless of the amount of FA utilized. It was further revealed that during the second-stage monomers almost polymerized on the surface of the seeds and formed the shell phase. The particle size and the obtained PDI exhibited that the FA phase was polymerized as a block.

Particle diameters were also determined from the height profile (Fig. 4) on latex dry films by scanning force microscopy (SFM) working in the tapping mode, which means that the force exerted on the film by the cantilever was kept constant during scanning. The diameter of the particles was obtained from the average distance between the center of two adjacent particles [represented by the triangles in



(a)



(b)

Figure 4 (a) SFM top view (size: $2 \times 2 \mu\text{m}^2$) of a Run 6 latex film and (b) height profile taken along the line shown on the top view image.

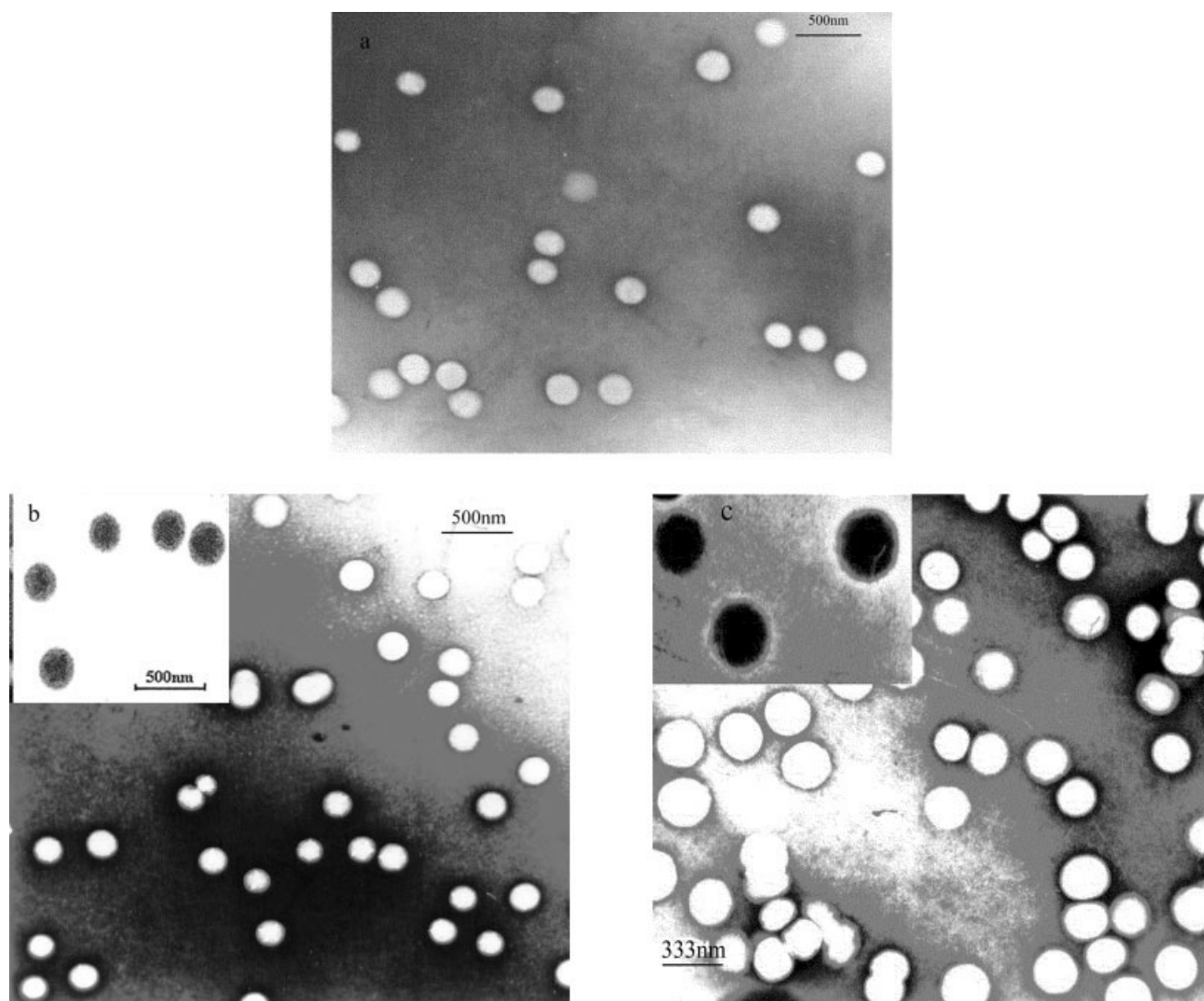


Figure 5 Transmission electron graphs of the core-shell latex particles from Run 2 (a), Run 6 (b), and Run 7 (c), and the inserted ones were amplified and phase-inverted.

Fig. 4(b)], using the SFM software. It was found that the values of D_w were smaller than those measured by PCS. As we know, the size of the particles measured by PCS refers to the hydrodynamic diameter, which includes the solvation layer around the latex particles. Furthermore, volume-shrink effect of latex during film-forming process will decrease the size of latex particles. Besides the determination of the particle diameter, SFM allows one to appreciate the shape and the polydispersity of the particles. SFM images revealed that all particles investigated in this study were spherical with a very low polydispersity in size and that no second nucleation had appeared.

As a mean to establish how MMA/nBA/FA was able to polymerize to form monomodal particles, TEM images were collected. Figure 5 illustrated TEM images of Run 2 (MMA/nBA), Run 6 (MMA/nBA/FA, 4.0 wt %), and Run 7 (MMA/nBA/FA,

6.5 wt %). As shown in Figure 5(a), MMA/nBA colloidal particles existed as monomodal entities with no considerable electron density changes. On the other hand, the incorporation of 4.0 and 6.0 wt % FA [Fig. 5(b,c)] resulted in the particles of similar size, but the particles exhibited two distinguish electron density changes. The presence of the long perfluoroalkyl side chains resulted in intraparticle phase separation with highly electron dense regions existing near the exterior of the particles. The thickness of darker shell was evaluated to about 20–30 nm, and the spherical as well as irregular spherical morphology of core were observed too. FA diffused at a slower rate than MMA and nBA, which gave rise to the synthesis of monomodal particles possessing FA blocks near the exterior of the MMA/nBA/FMA particles.²² The TEM images reinforced the findings described in DSC, thus confirming that FA polymerized

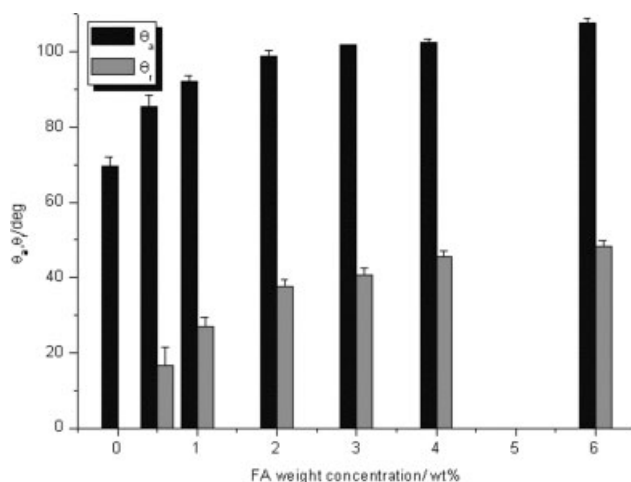


Figure 6 The plot of aqueous contact angles of FA copolymer latex films against the FA weight concentration.

as a blocky, phase-separated entity onto the exterior of existing MMA/nBA colloidal particles. And the second T_g at higher temperature was corresponded to the microphase enriched with perfluoroacrylate.

Contact angle measurements

With these data in mind, it was of interest to elucidate how these differences affected surface macroscopic properties. For that purpose, we measured the aqueous contact angles as function of FA, and the results were plotted in Figure 6. A gradual increase in the advancing (θ_a), and receding (θ_r) contact angles with increasing FA was seen. The presence of each copolymerized F-monomer altered the contact angles (θ_a and θ_r) of a water drop at the surface for each film, which for MMA/nBA/FA, was above 90° and 18° , and for MMA/nBA, the contact angle was 69.5° and 0° . The F-containing polymer has low-surface-energy property, and incorporation of F-containing moieties into a polymer chain had been confirmed to be effective for raising the hydrophobicity of film's surface as argued from the increase in contact angles.

Apparently, delay of FA addition in the second stage would favor the perfluorinated side chains rich in the shell and reduce the possibility to be buried, thus, excellent alignment of the $-\text{CF}_3$ groups on the surface was obtained during film-formation process. This was consistent that the advancing contact angles were increased with FA weight concentrations because θ_a was more sensitive to the nonwetable portions on a surface.

The receding contact angles, θ_r , were sensitive to the polar, more wettable portions of the surfaces. And the content of polar groups occupied at the film/air interfaces decreased with FA increasing. Thus, the opportunity of water droplets adhering to

the stand polar portions on the surfaces was gradually decreased during dewetting process, namely, θ_r existed significant improvement depending on the weight concentration of FA in the formulation.

Although an obvious decrease of CA hysteresis (which is defined as the difference between θ_a and θ_r) was found compared F-containing films with the fluorine-free, the large hysteresis was still observed at the resulting surfaces, which suggested that the surfaces were not dense enough to prevent water molecules penetrating. The penetrate water molecules could associate with either the polar $-\text{C}=\text{O}$ moieties or amide-ester through hydrogen bonding. Such associated water molecules could rearrange the structure of the surfaces and reduce surface hydrophobicity. Therefore, the lower receding angles were observed. Such results implied that water penetration could indeed induce structural rearrangement at the nonstick surface.

CONCLUSIONS

A series of core-shell latex particles containing perfluoroacrylate rich in the shell were successfully synthesized under monomer-starved condition via semicontinuous emulsion polymerization. All particles were core-shell spherical with a very low polydispersity in size. Further experiments were carried out to observe the effect of particle morphology on surface properties. The presence of FA in MMA/nBA colloidal systems results in a surface phase separation. As increasing FA, the latex films exhibited similar advancing contact angle of 100° , there existed significant improvement in the receding CA depending on the weight concentration of FA in the formulation.

References

- Lynn, M. M.; Worm A. T. In *Encyclopedia of Polymer Science and Engineering*, Vol. 7; Mark, H. F.; Bikales, N. M.; Overberger, C. G.; Menzes, G., Eds., 2nd ed.; Wiley: New York, 1987; p 256.
- Boutevin, B.; Diaf, K. O.; Pietrasanta, Y.; Taha, M. *J Polym Sci Part A: Polym Chem* 1986, 24, 3129.
- Yang, S.h.; Wang, J.; Ogino, K.; Valiyaveetil, S.; Ober, C. K. *Chem Mater* 2000, 12, 33.
- Alessandrini, G. M. A.; Castelvetro, V.; Ciardelli, F.; Peruzzi, R. *J Appl Polym Sci* 2000, 76, 962.
- Dreher, W. R.; Jarrett, W. L.; Urban, M. W. *Macromolecules* 2005, 38, 2205.
- Movchan, T.; Plotnikova, E.; Redina, L.; Gal'braikh, L.; Ys'yarov, O. *Colloid J* 2003, 65, 47.
- Barthelemy, P.; Tomao, V.; Selb, J.; Chaudeir, Y.; Pucci, B. *Langmuir* 2002, 18, 2557.
- Huang, Z.; Shi, C.; Xu, J.; Kilic, S.; Enick, R.; Beckman, E. *Macromolecules* 2000, 33, 5437.
- Linemann, R. F.; Malner, T. E.; Brandsch, R.; Bar, G.; Ritter, W.; Mulhaupt, R. *Macromolecules* 1999, 32, 1715.

10. Landfester, K.; Rothe, R.; Antonietti, M. *Macromolecules* 2002, 35, 1658.
11. Mawson, S.; Johnston, K. P.; Betts, D. E.; McClai, J. B., DeSimone, J. M. *Macromolecules* 1997, 30, 71.
12. Yang, T. T.; Peng, H.; Cheng, S. Y. *J Fluorine Chem* 2005, 126, 1570.
13. Cheng, S. Y.; Chen, Y. J.; Wang, K. L. *Acta Polym Sin* 2002, 5, 560.
14. Ha, J. W.; Park, I. J.; Lee, S. B. *Macromolecules* 2005, 38, 736.
15. Li, K.; Wu, P.; Han, Z. W. *Polymer* 2002, 43, 4079.
16. Marion, P.; Beinert, G.; Juhue, D.; Lang, J. *J Appl Polym Sci* 1997, 64, 2409.
17. Cheng, S. Y.; Chen, Y. J.; Chen, Z. G. *J Appl Polym Sci* 2002, 85, 1147.
18. Ha, J. W.; Park, I. J.; Kim, D. K.; Kim, J. H.; Lee, S. B. *Surf Sci* 2003, 328, 532.
19. Zhang, C. C.; Chen, Y. J. *Polym Int* 2005, 54, 1027.
20. Schmidt, D. L.; Brady, R. F.; Lam, K.; Schmidt, D. C.; Chaudhury, M. K. *Langmuir* 2004, 20, 2830.
21. Schmidt, D. L.; DeKoven, B. M.; Coburn, C. E.; Potter, G. E.; Meyers, G. F.; Fischer, D. A. *Langmuir* 1996, 12, 518.
22. Dreher, W. R.; Jarrett, W. L.; Urban, M. W. *Macromolecules* 2005, 38, 2205.